OPTOELECTRONICS AND ADVANCED MATERIALS – RAPID COMMUNICATIONS Vol. 4, No. 10, October 2010, p. 1568 - 1571

Structure and Mössbauer measurements on $SnSe_2$ bulk and thin films

I. BIBICU[*], A. LŐRINCZI, A. VELEA, F. SAVA, M. POPESCU
National Institute R&D of Materials Physics, Bucharest-Măgurele, 077125, Romania

Thin films samples of $SnSe_2$ deposited by PLD and PED have been prepared and studied by XRD and Mössbauer spectroscopy. The films are crystalline with a major phase of $SnSe_2$ and minor phase of amorphous $SnSe_2$. An oxidation process lead to the appearance of a thin layer of SnO_2 on the surface of the PLD samples.

(Received September 15, 2010; accpeted October 14, 2010)

Keywords: $SnSe_2$, Mössbauer measurements: transmission and backscattering method, XRD, PLD, PED

1. Introduction

Nanomaterials based on various chalcogenides have strong implications in many applications including biology and medicine for cancer treatment [1-3], typhoid fever [4] and plant growth promotion [5].

Tin chalcogenides SnX_2 and SnX, where X=S, Se or Te, present a particular interest for their electronic properties [10, 11] and applications in gas sensors. They belong to amorphous and glassy chalcogenides, materials which are sensitive to light and other radiations.

The tin chalcogenides – SnS and SnSe – have been prepared by direct vapour transport technique [6]. More complex films of Sn-Sb-S [7], Pb-Sn-Te [8] and amorphous Sn-Sb-Se-Te [9] have been prepared and studied very recently.

The state of tin in these materials is important for understanding of the sensing effect and improvement of the sensor performances. Mössbauer spectroscopy is a widely used technique for the investigations of the electronic structure or chemical bonding in solids [12-14]. ^{119}Sn Mössbauer spectroscopy is a very efficient tool for probing the local environment of tin atoms in the as-prepared chalcogenides and their intercalation products [11, 15]. The system Sn-Se is poorly studied although its semiconducting properties deserve a high interest. Thin films of tin-selenium have numerous applications in photovoltaic systems and in memory switching devices.

In this communication we report on the preparation of $SnSe_2$ bulk and thin films and applied XRD and Mössbauer technique for the investigation of bulk and thin films of $SnSe_2$ chalcogenide. Mössbauer measurements were performed by transmission (TMS), respectively conversion electron spectroscopy (CEMS). By CEMS spectroscopy surfaces, coatings and thin films containing Sn can be studied on substrates and to various depths up to 1000 nanometers.

2. Experimental

$SnSe_2$ bulk samples were prepared by mixing corresponding amounts of Sn and Se powder (high purity grade) in sealed quartz ampoule. The synthesis was carried out by heating the vacuum evacuated and loaded ampoule for 20 h at 730 ^{0}C in a tubular furnace, in a similar manner as in [16]. The ampoule has been periodically shaked in order to get homogeneous compositions. At the end of the synthesis time, the ampoule was quenched in a mixture of ice and water. Ingots of 1.9 cm in diameter, 4 cm in length and of grey colour were obtained. The ingots were cut in several disc-shaped to prepare the targets for deposition and samples for XRD and Mössbauer measurements.

The pulsed laser deposition (PLD) deposition was carried out with a KrF^* excimer laser [16]. The laser source generated pulses having the wavelength $\lambda = 248$ nm with pulse duration $\tau_{FWHM} > 7$ ns and 1 Hz repetition rate. The maximum output power was 110 mJ/pulse corresponding to a fluence of ~ 3.6J/cm^2 for a laser spot of 3 mm^2. As an alternative to pulsed laser deposition, pulsed electron deposition (PED) was made with electron beams produced in channel-spark discharge [17]. A pulsed electron beam was produced having about 100 ns FWHM and a fluence of 1-3 J/cm^2, depending on the applied voltage. The typical discharge voltage was -15kV and the repetition rate was 1Hz. The beam is polyenergetic with electron energies in the range 0-15 keV. The working gas was argon at a pressure of around 10^{-2} mbar. The rotating target is positioned at 45° to the electron beam direction. The substrate is placed at 4 cm distance from the target.

XRD measurements were carried out in a Bruker D8 Advance diffractometer, using $Cu_{K\alpha}$ radiation and a Göbel monochromator for the emerging beam.

Mössbauer measurements were performed at room temperature in transmission (TMS) and conversion electron Mössbauer spectroscopy (CEMS) using a conventional constant-acceleration spectrometer with an ^{119m}Sn source in a $CaSnO_3$ matrix. The Mössbauer samples for TMS had a superficial weight of 55 mg/cm^2 and a granulation better than 100 meshes. The CEMS measurements were conducted at a high degree of accuracy with a new detector, gas-flow proportional detector with a He-CH_4 mixture [18]. All CEMS spectra were recorded in perpendicular back-scattering geometry, i.e. with the incident γ-ray direction perpendicular to the film plane. The parameters of the Mössbauer spectra were calculated using a computer fitting program, which assumes a Lorentzian line shape. The isomer shifts were referred to α-Fe at room temperature. These measurements were performed for the first time in Romania.

3. Results and discussion

3.1 XRD results

The X-ray diffraction pattern recorded on polished discs is shown in Fig. 1. The identification of the crystalline phases in the ingot leads to the conclusion that the major phase consists of the $SnSe_2$ with hexagonal structure (Fiche No. 23-0602). A minor phase of $SnSe_2$ with cubic structure (Fiche No. 38-1055) was revealed. The background of the diffraction pattern indicates the presence of a significant content of amorphous phase as seen from the broad peak situated in the range: theta = $4 \div 13\ ^{o}$.

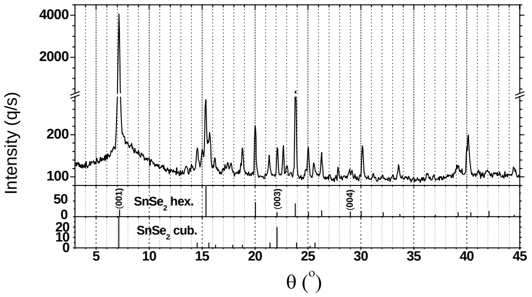

Fig. 1. X-ray diffraction pattern on the polycrystalline $SnSe_2$ ingot. Fraction of amorphous phase appears as a broad maximum below the first diffraction peak.

The X-ray diffraction diagrams taken on PLD and PED deposited films are shown in Fig. 2 and 3. In both cases the films show an amorphous structure.

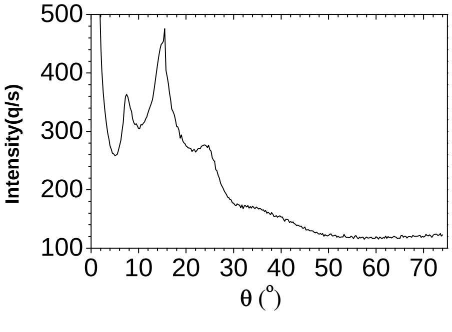

Fig. 2. X-ray diffraction pattern of the PLD films of $SnSe_2$.

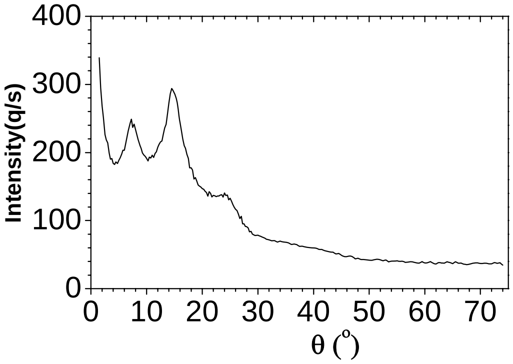

Fig. 3. X-ray diffraction pattern of the PED $SnSe_2$ film.

One observes some differences between the two diagrams. The PED films show larger maxima than the PLD films. This speaks in the favour of more order in the PLD films. The different kind of ordering in films could explain the propensity of oxygen to link to Sn and form a very thin layer of tin dioxide at the surface of the PLD films (see the Mössbauer results).

3.2 Mössbauer results

The Mössbauer spectra obtained on $SnSe_2$ bulk sample by TMS and CEMS are shown in Fig. 4. In Fig. 5 are presented the CEMS spectra obtained on $SnSe_2$ films deposited by two methods: PLD and PED deposition methods.

The spectral parameters of the Mössbauer components of each spectrum, presented in Figs. 4 and 5 are given in Table 1. In the table are indicated the compounds corresponding to each subspectrum.

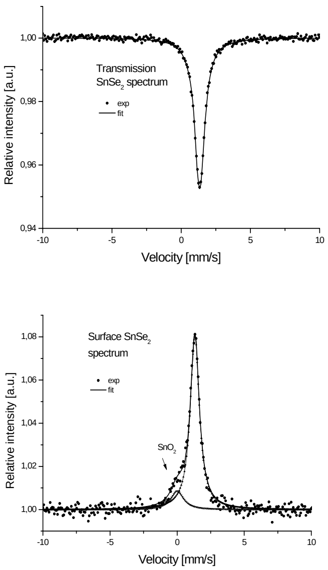

Fig. 4. Room temperature spectra of $SnSe_2$ bulk sample obtained by transmission (above) and conversion electron Mössbauer spectroscopy (below).

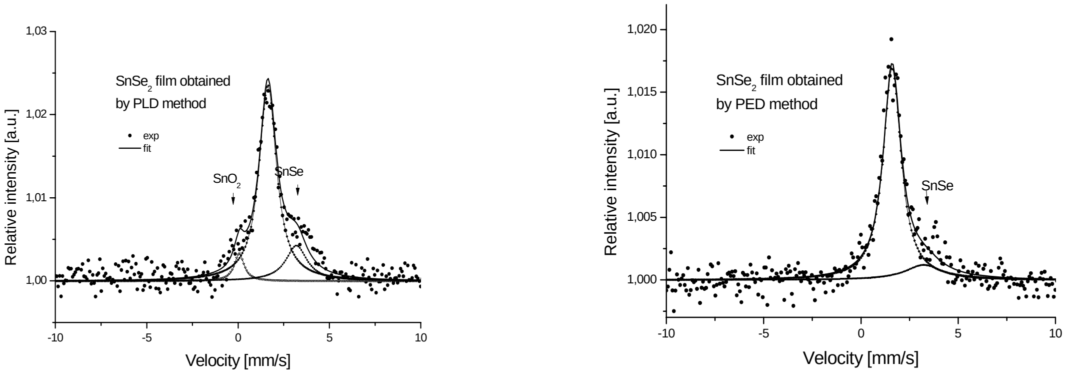

Fig. 5. Conversion electron Mössbauer spectroscopy spectra of SnSe$_2$ films obtained by PLD and PED deposition.

Table 1. The spectral parameters of the Mössbauer spectra presented in Figs. 4 and 5.

Sample	IS [mm/s]	W [mm/s]	ε %	A %	Assigned compound
SnSe$_2$ - bulk	1,43	0,90	4,78	100	SnSe$_2$
SnSe$_2$ - surface	1,40	0,86	8,07	87,09	SnSe$_2$
	0,05	1,16	0,86	12,91	SnO$_2$
SnSe$_2$ film obtained by PLD method	1,69	1,15	2,35	76,98	SnSe$_4$
	3,28	1,43	0,44	16,86	SnSe
	0,07	0,85	0,34	6,23	SnO$_2$
SnSe$_2$ film obtained by PED method	1,65	1,12	1,71	87,65	SnSe$_4$
	3,32	2,32	0,12	12,35	SnSe

where:

IS: Isomer shift in mm/s; errors ± 0.02
W: Line width in mm/s; errors ± 0.03
ε: Resonant effect in %; errors ± 0.05
A: Relative area of each subspectrum in %; errors ± 4

The Mössbauer parameters for SnSe$_2$ bulk samples are closed to those given in literature [11, 15, 19] for SnSe$_2$ and the line width values proves a well prepared compound. There is an oxidation process on its surface indicated by the presence of the SnO$_2$ oxide in the CEMS spectrum of the bulk sample. We consider an oxidation process in air atmosphere of the material. The thickness of thin films has been estimated to few nm [20].

The main component of the film spectra can be assigned to SnSe$_4$ [11] species by its isomer shift values: 1.69 and 1.66 s. These species are known as tetrahedral Zintl anions [SnSe$_4$] [21]. It is possible that studied films to be built from isolate SnSe$_4$ tetrahedra stabilized by atoms occupying intermediated positions [22]. A similar process met in mesostructured chalcogenide-based materials with long-range order and semiconducting properties using molecular building blocks, linked by metal ions and surfactant molecules [23]. The higher line width of the main component can be explained by the fact that SnSe$_4$ have tin environments slightly distorted from the basic tetrahedral symmetry [24].

The compound SnSe there is present in the both films in a small amount. The increased line width of the SnSe is explained by its quadrupole splitting with a value around 0.65 mm/s [11, 25]. The higher line width of the SnSe in the PLD film suggest a light structure distorsion of the SnSe compound with orthorhombic structure. The SnSe presence can be explained by the occurence of the reaction: $SnSe_2 \rightarrow SnSe + Se$ [25] in the deposition process. In the film spectrum obtained by PLD deposition we identify a third component, assigned to SnO$_2$ oxide. The oxide is localized at the film surface, the most probably, showing an oxidation in air atmosphere of the film.

We believe, according to our results, that by PED deposition method a better film is obtained. The arguments for the this affirmation are: a higher proportion of the main component, a lower line width of the main component, a lower line width of the SnSe component, the absence of the SnO$_2$ oxide.

4. Conclusions

Bulk and thin film samples of $SnSe_2$ chalcogenide have been prepared and studied by XRD and transmission Mössbauer spectroscopy (TMS), respectively, conversion electron Mössbauer spectroscopy (CEMS).

The Mössbauer parameters for $SnSe_2$ bulk samples are the same as in literature. There is an oxidation process on their surface indicated by the presence of the SnO_2 oxide in the CEMS spectra.

The structure of main component of the films it is possible to be built from isolate $SnSe_4$ tetrahedra stabilized by atoms occupying intermediated positions. SnSe there is present in the both films in a small amount. On the film obtained by PLD deposition we found SnO_2 oxide.

Acknowledgements

The authors are grateful to Dr. Gabriel SOCOL for preparing the PLD films, and to Dr. Magdalena NISTOR for preparing the PED films.

This work was supported by National Authority for Scientific Research (ANCS) under Core Program Project PN09-45.

References

[1] A. Kumar Singh, A. Pandey, R. Rai, M. Tewari, H. P. Pandey, Digest J. Nanomat. Biostr. **3**(3), 135 (2008).
[2] A. Pandey, A. K. Singh, S. K. Maurya, R. Rai, N. S. Shukla, Digest J. Nanomat. Biostr. **3**(3), 141 (2008).
[3] S. Shrivastava, Digest J. Nanomat. Biostr. **3**(4), 257 (2008).
[4] R. Mitra, Digest J. Nanomat. Biostr. **4**(1), 109 (2009).
[5] V. K. Mishra, A. Kumar, Digest J. Nanomat. Biostr. **4**(3), 587 (2009).
[6] B. B. Narya, A. K. Dasadia, M. K. Bhayani, A. J. Patel, A. R. Jani, Chalc. Lett. **6**(10), 549 (2009).
[7] A. Gassoumi, M. Kanzari, Chalc. Lett. **6**(4), 163 (2009).
[8] M. Abdel Rafea, F. S. Terra, M. Mounir, R. Labusch, Chalc. Lett. **6**(3), 115 (2009).
[9] R. Chandler, R. Tangaraj, Chalc. Lett. **5**(10), 229 (2008).
[10] T. J. Wieting, M. Schlüter, Electron and Phonons in Layered Crystal Structures, Reidel, Dordrecht (1979).
[11] P. E. Lippens, Physical Review B**, 60**, 4576 (1999).
[12] R. L. Mössbauer, Z. Physik, **151,** 124 (1958).
[13] G. J. Long, Mössbauer Spectroscopy Applied to Inorganic Chemistry, Plenum, New York (1984).
[14] A. G. Maddock, Moessbauer Spectroscopy: Principles and Applications of the Techniques*,* (Horwood Chemical Science Series), Horwood (1997).
[15] A. Svane, N. E. Christensen, C. O. Rodriguez, M. Methfessel, Physical Review B **55,** 12572 (1997).
[16] M. Popescu, A. Velea, F. Sava, A. Lőrinczi, A. Tomescu, C. Simion, E. Matei, G. Socol, I. N. Mihailescu, A. Andonie, I. Stamatin, Phys. Status Solidi, **A 207**(3), 516 (2010).
[17] G. Müller, M. Konijnenberg, G. Krafft, C. Schultheiss, Science and Technology of Thin Film, World Scientific Publ. Co. PET. LTD, 89 (1995).
[18] I. Bibicu, G. Nicolescu, C. Cretu, Hyperfine Interactions*,* **192**, 85 (2009).
[19] P. E. Lippens, J. Oliver-Fourcade, J. C. Jumas, Hyperfine Interactions*,* **126**, 137 (2000).
[20] G. P. Huffman, Applications of Mössbauer Spectroscopy, pp. 189-207 Academic Press Inc, New-York, (1980).
[21] P. N. Trikalitis, R. K. Kasthuri, T. Bakas, M. G. Kanatzldis, Nature, **410**, 671 (2001).
[22] G. Akinocho, P. Houenou, S. Oyetola, R. Eholie, J. C. Jumas, J. Oliver-Fourcade, M. Maurin, Journal of Solid State Chemistry*,* **93**, 336 (1991).
[23] P. N. Trikalitis, T. Bakas, M. G. Kanatzldis, J. Am. Chem. Soc., **127**, 3910 (2005).
[24] T. Birchall, R. C. Burns, L. A. Devereux, G. J. Schrobilgen, Inorg. Chem., **24**, 890 (1985).
[25] G. A. Bordovskii, R. A. Castro, A. V. Marchenko, P. P. Seregin, Glass Physics and Chemistry*,* **33**, 467 (2007).

---

*Corresponding author: bibicu@infim.ro